Jisha Joseph “Self-assembly of structurally diverse phosphomolybdates: synthesis, structure and properties.” Thesis. Research and Post gradute Department of Chemistry, St. Thomas college (autonomous), University of Calicut, 2020.

CHAPTER VI

Investigations using composites based on APM

Summary

In this chapter, two binary composites of ammonium phosphomolybdate (APM) with polyaniline (PAni) and poly (N-methylaniline) (PNMAni) have been synthesized and characterized. The composite of APM with poly (N-methylaniline), APM/PNMAni has not been reported in literature so far. The electrochemical behavior of APM/PAni and APM/PNMAni were investigated using cyclic voltammetry and the band gap energy was calculated using DRS data. Further, the role of these composites in the removal of hexavalent chromium from aqueous solution was explored. The removal of Cr(VI) from aqueous solution was monitored using UV-Vis spectroscopy. It was observed that APM/PNMAni exhibited enhanced ability to remove Cr(VI) as compared to APM and APM/PAni.

VI.1. Introduction

Composite materials have drawn the attention of researchers consistently, on account of their enhanced properties in comparison to its components. Keggin-type phosphomolybdates (PMOs) are a well defined sub-class of heteropolyanions with multifaceted peculiarities [1-2]. A number of polynary composites of Keggin-type PMOs have been developed recently with attractive applications as high performance sensors, supercapacitors, catalysts and electrodes [3-6]. A review of such binary composites reported in the past decade has been summarized in Table VI.1. From the table it is evident that PMo_{12} is an active composite component with polymers, reduced graphene oxide, and Bi_2O_3, exhibiting excellent properties [7-10]. It is also notable that, these composites have not been used to remove carcinogenic environmental pollutant inorganic hexavalent Cr(VI) from aqueous solutions. Only a few groups have reported the catalytic property of reduced phosphomolybdates *viz.* $\{P_4Mo_6\}$ cluster based solids in the reduction of Cr(VI) [11-13].

Ammonium phosphomolybdates (APM), $\{NH_4\}_3[PMo_{12}O_{40}].xH_2O$ is an established yellow colored cluster based solid, which is well known as a cesium ion absorber [14-15]. The synthesis, characterization and application of APM in removal of dye moieties have been described in Chapter V. In order to improve the properties of APM, it is convenient to convert it into a composite form with suitable materials. However, the binary composites containing PMOs are comparatively less studied (refer Table VI.1). Therefore, in this chapter, an attempt has been made to synthesize and characterize APM composites with two polymers *viz.* polyaniline and poly (N-methylaniline) namely, APM/PAni and APM/PNMAni respectively. The electrochemical behavior of the synthesized composites

was explored by means of three electrode system using 1 mM $K_4[Fe(CN)_6]$ in 0.1 M KCl as supporting electrolyte. Band gap energy of APM as well as the synthesized composites was calculated from UV-Vis diffused reflectance spectra applying Kubelk-a-Munk F(R) function in Tauc method [16, 17]. The optical band gap of composites was increased considerably compared to that of APM, which is significant in solar energy cells. Besides, the role of APM and its synthesized composites in the removal of hexavalent chromium from aqueous solution has also been investigated.

Table VI.1. A preview of PMo_{12} based composites reported in the past decade.

Sl. No.	Composite Composition	Synthesis (method)	Properties/ applications	Refere-nces
1	$H_3PMo_{12}O_{40}$ & Poly vinyl alcohol	Prepared by using layer-by-layer assembly technique to form the multilayer films	Visible light photochromism	[7]
2	$H_3PMo_{12}O_{40}$ & Polyaniline	By stirring solutions of aniline, APS and $H_3PMo_{12}O_{40}$ dissolved/dispersed in DDW together	As electrocatalysts for the reduction of bromates	[8]
3	$H_3PMo_{12}O_{40}$ & Reduced graphene oxide	Reduced graphene oxide was dispersed in DI water. 1% ethylene glycol and an aqueous solution of $H_3PMo_{12}O_{40}.nH_2O$ was added to the rGO and sonicated	Electrochemical oxidation of nitrite ions	[9]
4	$Na_3[PMo_{12}O_{40}]$ & Agarose composite thin film	To Agarose solution in water PMo_{12} was added. After vacuum defoamation process, the mixed solutions were cast on ITO glass substrates, followed by gelating, and drying	Visible light photochromism	[18]
5	Phosphomolybdate	Tetrabutylammonium salts of	Oxidative	[19]

	& Carbon nanomaterial	PMOs were synthesized and it is immobilized on single walled carbon nanotubes	electrocatalysis	
6	APM & polyacrylonitrile	Not reported	Pre-concentration and separation of Rb(I) ion from salt lake brine	[20]
7	APM & polyacrylonitrile	To APM dissolved in DMSO with Tween 80 as surfactant, Pan was added. To get spherical beads, the composite mixture was fed into a syringe with a needle and injected into DW dropwisely	Selective removal of Cesium from water	[21]
8	APM & polyacrylonitrile	20 g of AMP and 0.8 g of Tween 80 were combined with 100ml of DMSO. After stirring the solution for 1 h at 50^{o}C, 8 g of PAN was added and stirred for 5 h at 50^{o}C to obtain composite mixture	Removal of cobalt, strontium and cesium from radioactive laundry wastewater	[22]
9	$H_3PMo_{12}O_{40}$ & Chitosan	To 5 wt% chitosan solution 20% w/v of PMA was added with a cross linking agent	Enhanced thermal stability and mechanical properties	[23]
10	$H_3PMo_{12}O_{40}$ & polyacrylamide	Different solutions of PMA and Polyacrylamide in deionized water and mixed with constant stirring	Photochromic properties	[24]
11	$H_3PMo_{12}O_{40}$ & Chitosan	By drop wise addition under sonication of CTAB in EtOH to an aqueous solution of $H_3PMo_{12}O_{40}$. An equivalent volume of chitosan solution was added under sonication producing the composite	Antimicrobial activity	[25]
12	APM & Poly acrylonitrile	To hot DMSO and Tween 80 APM powder was added with	The effect of gamma irradiation on the ion	[26]

		stirring. PAN was added and stirred for 6 hours. The mixture was sprayed with compressed air into a large excess of deionised water through a confined jet nebuliser	exchange properties of caesium-selective AMP-PAN composites under spent fuel recycling conditions	
13	$H_3PMo_{12}O_{40}$ & Oligomeric ionic liquid	0.3 mmol of oligomeric ionic liquid was dissolved in deionized water and subsequently an aqueous solution of phosphomolybdic acid in 10 ml of H_2O was added to under ultrasonic radiation for 2x15 min to obtain products	Used as heterogeneous catalyst for the oxidation of cyclohexane under solvent free conditions	[27]
14	$H_3PMo_{12}O_{40}$ & Polymethylmatha-crylate (PMMA)	$H_3PMo_{12}O_{40}$ dissolved in ethanol poured to PMMA dissolved in DMF	Photocatalytic property	[28]
15	$[(C_4H_9)_4N]_3$ $[PMo_{12}O_{40}]$ & graphene	Solution-phase reaction method	Advanced cathode for high performance lithium ion batteries	[29]
16	$Cs_3PMo_{12}O_{40}$ & Bi_2O_3	Dissolution-precipitation method	Photocatalytic activity under visible-light irradiation	[30]
17	$[PMo_{12}O_{40}]^{3-}$ & polyamidoamine	Layer by layer electrostatic assembly technique	Electrocatalytic activities regarding methanol oxidation by depositing Pt micro nano clusters on the surface of the composite	[31]

VI.2. Experimental Section

VI.2.1. Synthesis of APM/Polymer composite

The synthesis of composites based on APM *viz*. APM/PAni and APM/PNMAni was carried out as follows:

To a stirring solution of 20 ml ammonium heptamolybdate (0.03 M, Merck, 99%), 10 ml of disodium hydrogen phosphate dihydrate (0.2 N, Aldrich, 99%) in 8 ml conc. HNO_3 was added. 0.5 ml of Aniline/ N-methyl aniline was added in small aliquots to the stirring solution. The contents were stirred for 18 hours and the resultant dark green powder was washed with water. The products thus obtained were dried for 20 hours at 50°C.

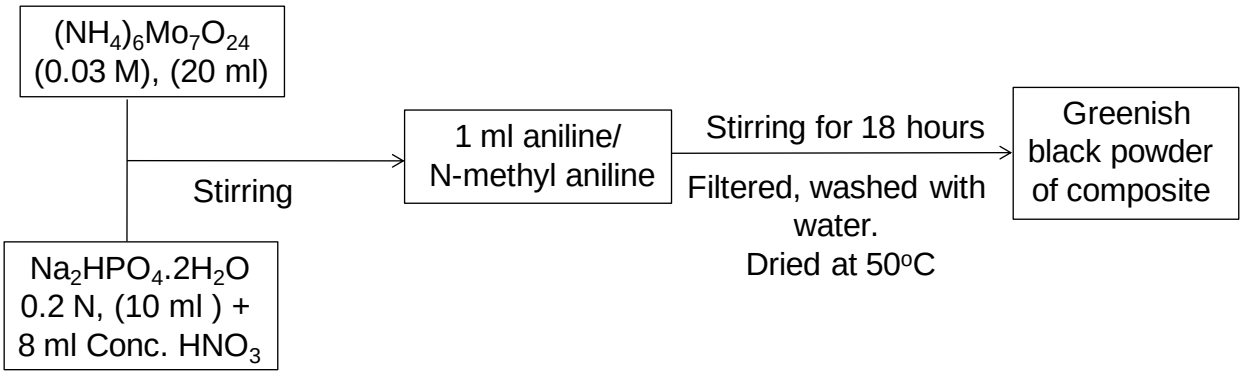

Scheme VI.1. Procedure for the synthesis of APM/PAni and APM/PNMAni.

VI.2.2. Synthesis of Polymers

In order to ascertain the formation of composites; powder X-ray diffraction (PXRD) patterns of composites were compared with those of polymers and APM. The preparation of APM has already been discussed in Chapter V. The methodology employed for the preparation of polymers was similar to that reported in literature by Ganesan *et. al*. [32].

Initially two different solutions were prepared. Solution A consisted of 0.05 mol of aniline/ N-methylaniline in 35 ml of 3 M HCl and solution B was prepared by dissolving 0.05 mol of ammonium persulphate in 50 ml of distilled water. The two solutions were stirred separately for 15 minutes. Then solution A was added to the stirring solution of B drop wise under ice-cold condition. The stirring was continued for 2 hours. The dark green resultant solution was filtered and the product thus obtained was filtered, washed with distilled water and ethanol and dried for 12 hours in oven at 50^{o}C.

VI.3. Characterization

Synthesized APM/PAni and APM/PNMAni composites were characterized using techniques discussed under Section II.2.2 in Chapter II. The presence of Cr(VI) ions was detected with respect to the change in intensity of absorption peaks using UV-Vis spectroscopy (Shimadzu UV-Visible 1800 double beam spectrophotometer).

VI.4. Results and discussion

VI.4.1. Characterization of APM/PAni

The FTIR spectrum of APM/PAni composite showed the presence of bands in the region 1100-550 cm^{-1} which are characteristic of Keggin type heteropoly anions (Figure VI.1a). The peaks at 1066, 970 and 881 cm^{-1} were assigned to γ_{as} (P-O$_a$), γ_{as}(Mo-O$_d$) and γ_{as}(Mo-O$_b$-Mo) respectively [33]. The peaks at 1113 and 807 cm^{-1} were due to the aromatic C-H out-of-plane bending and aromatic C-H in-plane bending vibrations respectively [34]. A well defined peak at 1349 cm^{-1} could be assigned to C=N stretching of secondary amines. Peaks at 1434 and 1533 cm^{-1} were attributed to C=C stretching vibrations of benzenoid ring and

quinonoid ring respectively. The spectrum showed a broad band in the region of 3238–3507 cm^{-1} which is associated with the N-H stretching vibrations of secondary amines [34].

In order to ascertain the formation of composite, PXRD pattern of composite was compared with that of polyaniline and APM. While PXRD of polyaniline showed broad peaks at 2θ values 9°, 14.9°, 20.4°, 25.4°, 27.4° and 29.5° showing an amorphous nature; PXRD pattern of APM was found to be crystalline in nature and it matched well with JCPDS file no. 43-0315 indicating the formation of single-phasic cubic $\{NH_4\}_3[PMo_{12}O_{40}].xH_2O$ having lattice constant a = 11.67 Å. On the other hand, PXRD pattern of the composite APM/PAni showed characteristic peaks of APM along with some amorphous nature which confirmed the formation of APM/PAni composite (refer Figure VI.1b). SEM image of the resulting APM/PAni composite (Figure VI.1c) indicated the polydisperse nature of composite particles having irregular morphology. EDAX spectrum (Figure VI.1d) showed the peaks of carbon, nitrogen, phosphorous, molybdenum and oxygen at 0.277(Ka1), 0.392(Ka1), 2.014(Ka1), 2.518(Lβ2) and 0.525(Ka1) respectively (refer Table VI.2)

VI.4.2. Characterization of APM/PNMAni

The FTIR spectrum of PNMAni (Figure VI.2a) showed a band at 2314 cm^{-1} which was attributed to the stretching frequency vibrations of methyl group. The bands representing benzenoid and quinonoid rings appeared at 1500 cm^{-1} and 1576 cm^{-1} in APM/PNMAni composite with appreciable red shift from that of polymer [8] indicating the interaction of PNMAni chains with heteropolyacids. The position of the band at 873 cm^{-1} was attributed to the presence of para-substituted benzene rings ensuring the polymerization of NMAni in

composite [35]. A predominant band at 1304 cm^{-1} was associated with the C-N stretching vibrations of aromatic tertiary amines. Along with the bands of PNMAni, FTIR spectrum of the composite showed the characteristic bands of APM (in the region 1100-700 cm^{-1}) which confirmed the presence of Keggin polyanion in the composite.

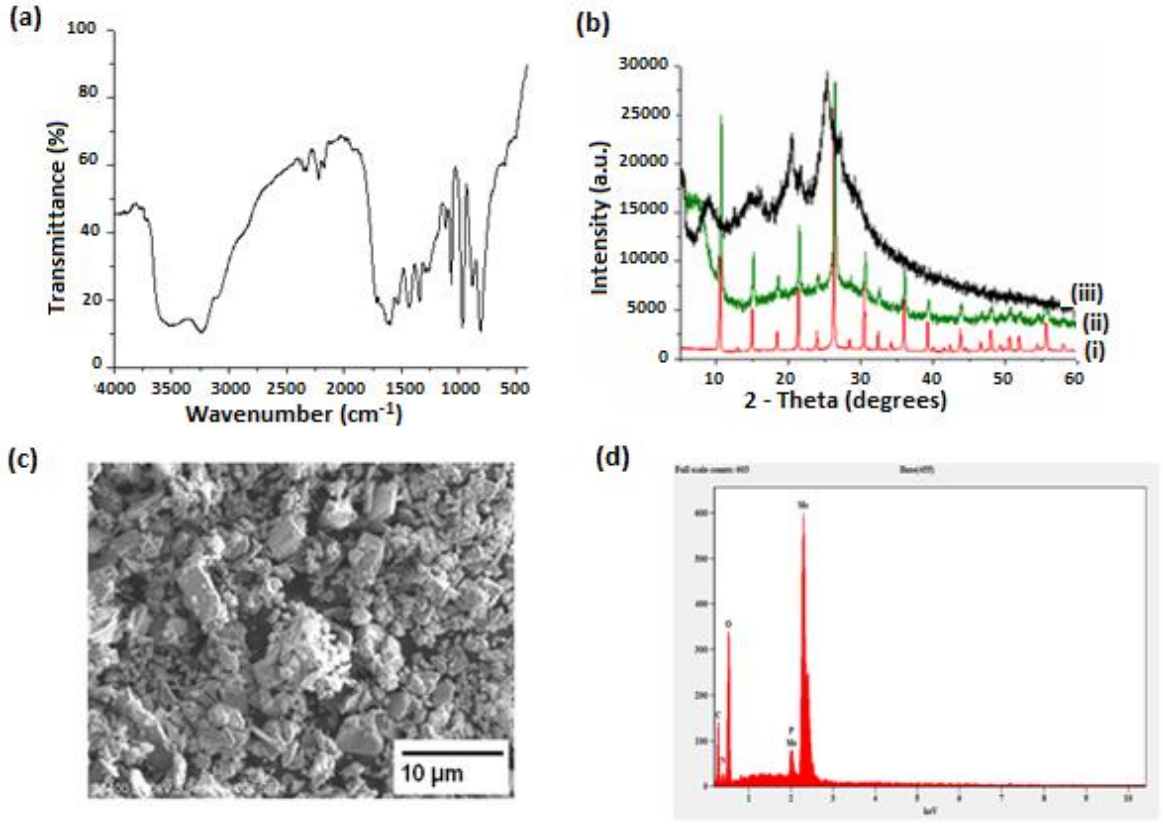

Figure VI.1. (a) FTIR spectrum of APM/PAni composite (b) PXRD pattern of (i) APM (ii) APM/PAni-composite (iii) PAni (c) SEM image and (d) EDAX spectrum of APM/PAni-composite.

PXRD pattern obtained for PNMAni, APM and APM/PNMAni composite are shown in Figure VI.2b. Since PNMAni shows amorphous nature, it does not have long-range atomic order. The PXRD pattern exhibited broad peaks at 2θ angles 10.4°, 18.3° and 23.3°

indicating its low degree of crystallinity. While the PXRD of composite showed an intermediate pattern of APM and PNMAni, with well defined peaks of APM at low intensities and an appreciable broadness of polymer, again confirming the formation of APM/PNMAni composite. SEM image of APM/PNMAni-composite is shown in Figure VI.3c. It showed the presence of polydispersed particles with irregular morphology. EDAX spectrum (Figure VI.2d) showed the peaks of carbon, nitrogen, phosphorous, molybdenum and oxygen at 0.277(Ka1), 0.392(Ka1), 2.014(Ka1), 2.831(Lg3) and 0.525(Ka1) respectively (refer Table VI.3).

Table VI.2. Weight % of elements present in APM/PAni from EDAX.

Element Line	Weight %	Atom %
C K	2.64	4.39
N K	19.76	28.16
O K	48.91	61.02
P K	1.07	0.69
P L	---	---
Mo L	27.62	5.75
Mo M	---	---
Total	100.00	100.00

Table VI. 3. Weight % of elements present in APM/PNMAni composite.

Element Line	Weight %	Atomic %
C K	44.78	61.31
N K	6.84	8.03
O K	26.05	26.78
P K	0.14	0.08
Mo L	22.19	3.80
Total	100.00	100

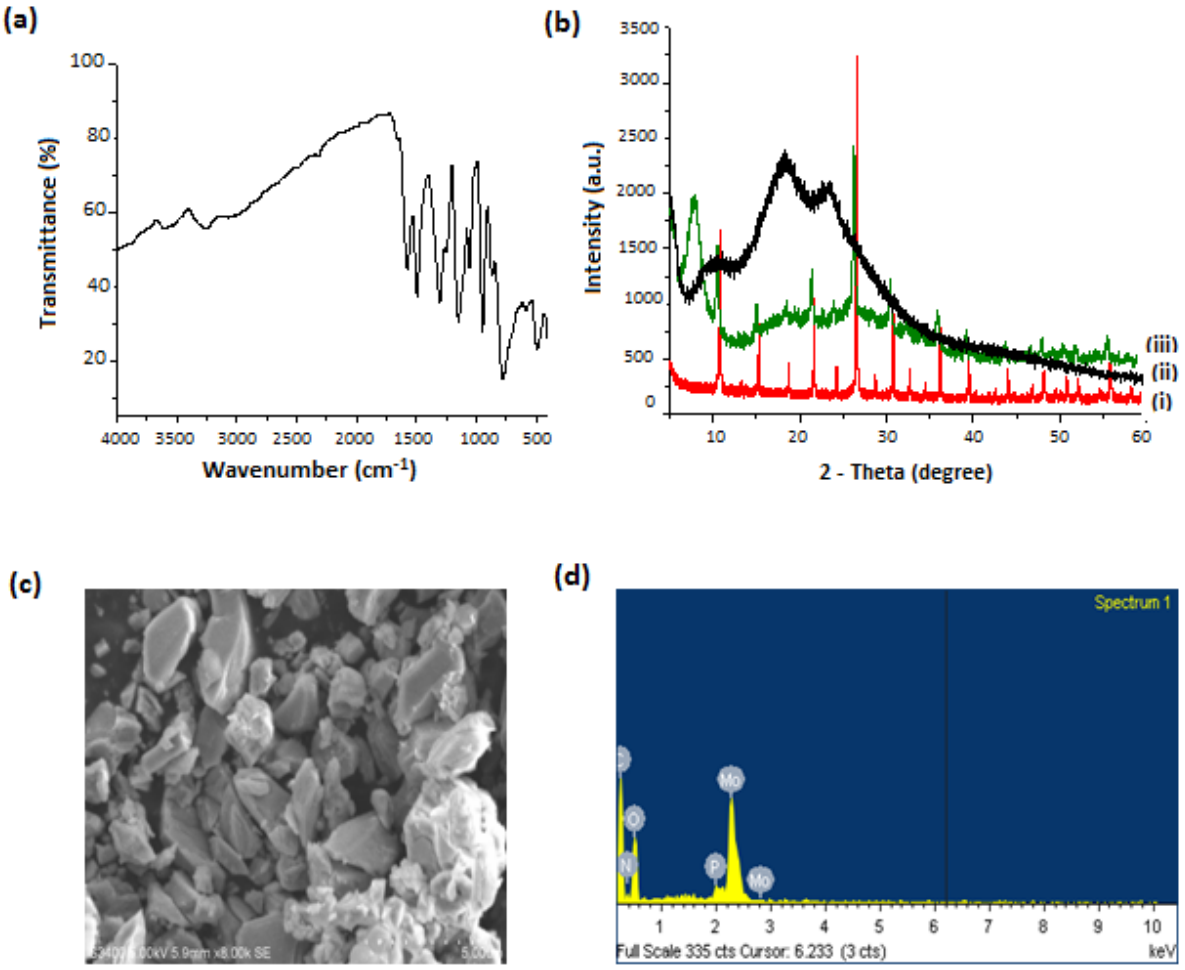

Figure VI.2. (a) FTIR spectrum of APM/PNMAni (b) PXRD pattern of (i) APM (ii) PNMAni and (iii) APM/PNMAni-composite (c) SEM image and (d) EDAX of APM/PNMAni-composite.

VI.5. Electrochemical behavior of composites

The effect of various electrolytes on the performance of composite electrodes was investigated by performing cyclic voltammetry experiments using a glassy carbon electrode (GCE) on which the synthesized APM and composites were coated separately. The electrochemical behavior of the composites in various electrolytes such as H_2SO_4 (0.1 M),

HCl (2 M), KOH (1 M) and $K_4[Fe(CN)_6]$ (1 mM) with a scan rate of 50 mVs^{-1} was investigated. Since PNMAni and PMo_{12} are unstable in basic solutions, desirable results did not obtained when KOH was used as the electrolyte. Among the others, best results were obtained when 1 mM $K_4[Fe(CN)_6]$ in 0.1 M KCl was used as supporting electrolyte. Figure VI.3 represents the cyclic voltammograms (CVs) of Bare GCE, APM, APM/PAni & APM/PNMAni in 1 mM $K_4[Fe(CN)_6]$ with a scan rate of 50 mVs^{-1} by applying potential range of -0.2 to +0.8V.

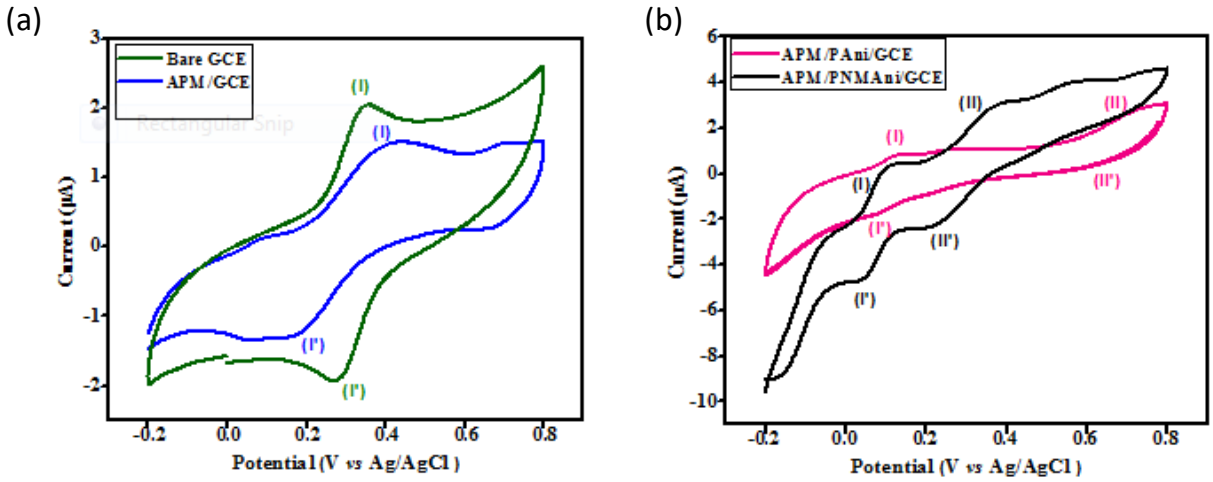

Figure VI.3. (a) CV of bare GCE and APM coated on GCE. (b) CV of APM/PAni and APM/PNMAni coated on GCE.

The small area of current at bare GCE and APM coated GCE represents the less available fast electrons at the electrode-electrolyte interface. The bare GCE gives a redox peak for $K_4[Fe(CN)_6]$ with mean peak potential E*1/2* = (*Epa* + *Epc*)*/2* at 0.317 V which can be attributed to Fe^{II}/Fe^{III} [36]. The redox couple obtained for APM at half wave potential 0.281 V could be attributed to Mo^{V}/Mo^{VI} electron process. It is noticeable that the E*1/2* obtained for Strandberg type PMOs were 0.087 and 0.072 V respectively for **1** and **2** described in

Chapter II. The different E*1/2* values obtained for Mo^{V}/Mo^{VI} electron process in $\{P_2Mo_5\}$ and $\{PMo_{12}\}$ could be because of the difference in the electron movement on account of different structural environment present in Strandberg and Keggin type PMOs.

The results showed that APM/PNMAni exhibits highest peak current response compared to APM and APM/PAni in the presence of a redox species 1 mM $K_4[Fe(CN)_6]$ in 0.1 M KCl. The redox peaks obtained for APM/PAni and APM/PNMAni at 0.228 V and 0.298 V respectively could be attributed to the Mo^{V}/Mo^{VI} electron process. The peaks obtained at 0.667 V for APM/PAni and 0.072 V for APM/PNMAni could be due to redox process involved in the polymeric chain of the composite. The appreciable peak shift towards lower potential value could be attributed to the electron donating behavior of methyl groups in poly(N-methyl aniline).

VI.6. Optical band gap energy (E_g) determination applying Kubelk- a–Munk (KeM or F(R)) function in Tauc method.

Optical band gap (E_g) determination was carried out using Tauc method, as discussed in Chapter II, under Section II.3.4.

Plots of F(R) and $(F(R)h\upsilon)^n$ (where n = ½ and 2 for indirect allowed transition and direct allowed transition respectively) versus hυ(eV) for APM, APM/PAni and APM/PNMAni composite are given in Figure VI.4, VI.5 and VI.6 respectively.

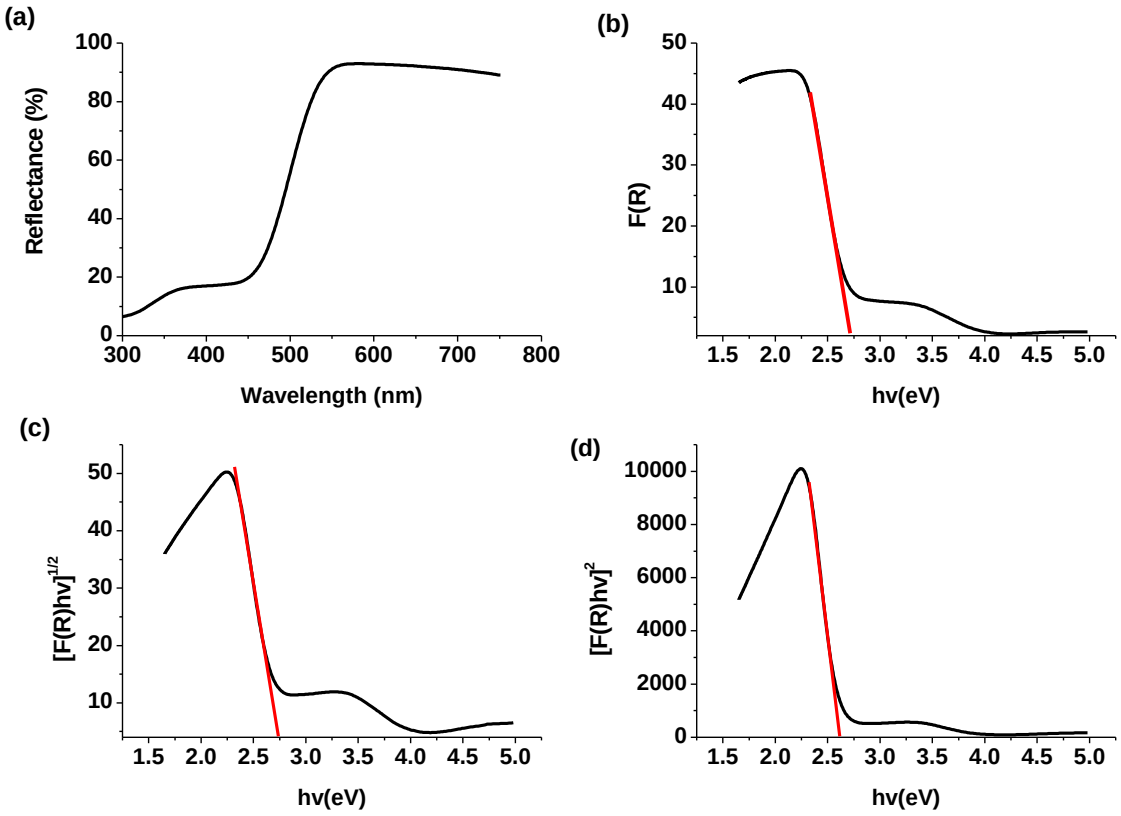

Figure VI.4. Plots of (a) Reflectance versus wavelength (b) F(R) versus hυ(eV), (c) $(F(R)h\upsilon)^{1/2}$ versus hυ(eV) and (d) $(F(R)h\upsilon)^{2}$ versus hυ(eV) for APM.

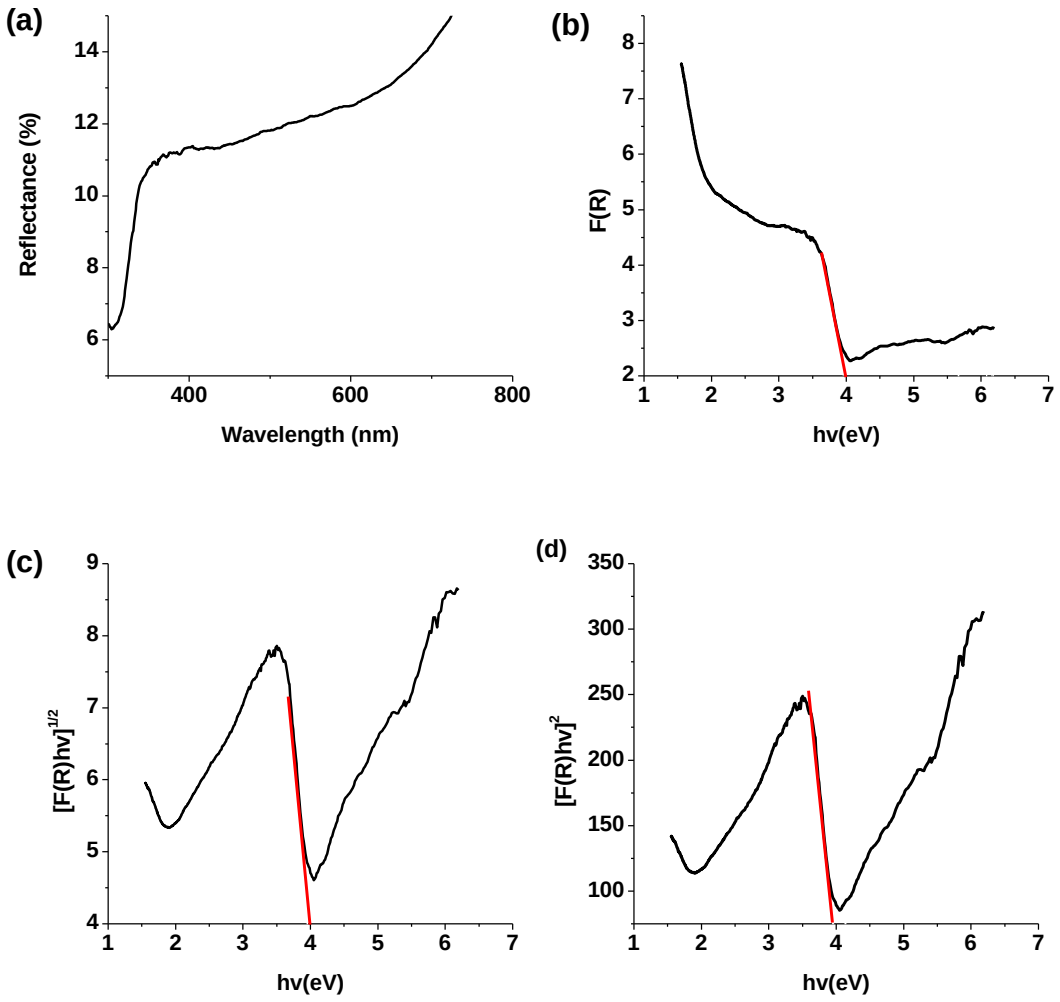

Figure VI.5. Plots of (a) Reflectance versus wavelength (b) F(R) versus hυ(eV), (c) $(F(R)h\upsilon)^{1/2}$ versus hυ(eV) and (d) $(F(R)h\upsilon)^{2}$ versus hυ(eV) for APM/PAni.

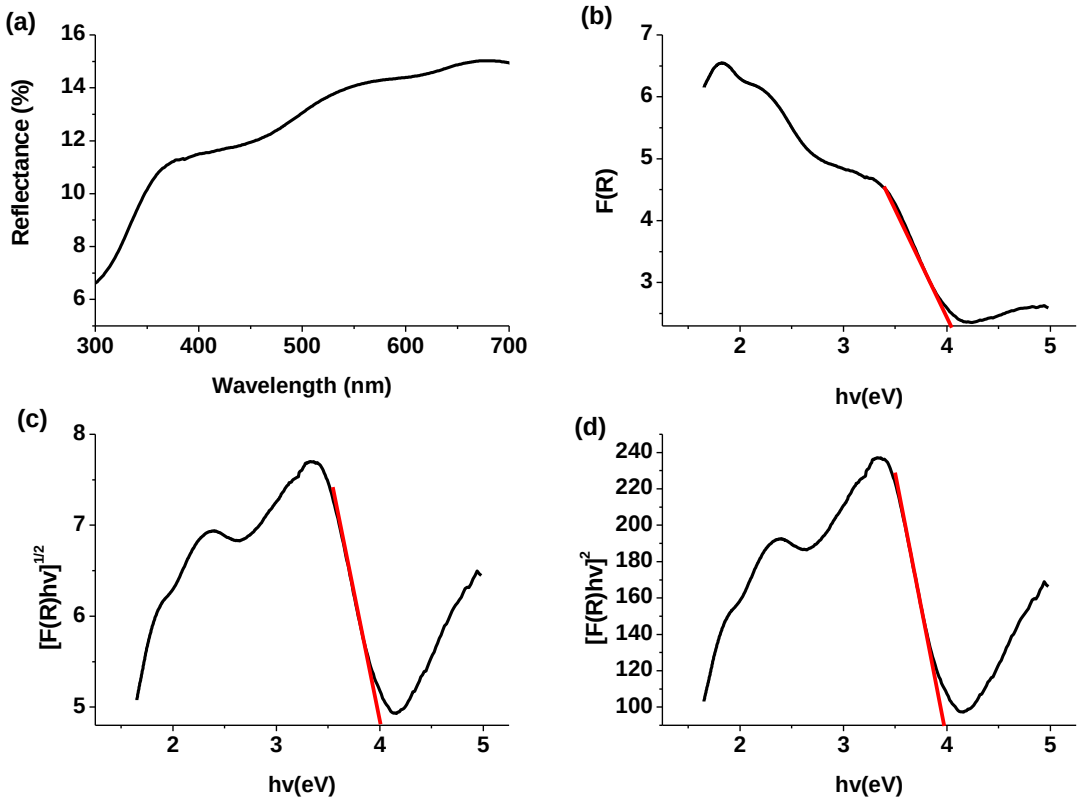

Figure VI.6. Plots of (a) Reflectance versus wavelength (b) F(R) versus hυ(eV), (c) $(F(R)h\upsilon)^{1/2}$ versus hυ(eV) and (d) $(F(R)h\upsilon)^{2}$ versus hυ(eV) for APM/PNMAni composite.

Table VI.4. Table tabulates the irrespective, allowed indirect and allowed direct band gaps of APM, APM/PAni and APM/PNMAni.

Solids	$[F(R)\ h\upsilon]^2$ (allowed direct Band gap energy in eV)	$[F(R)\ h\upsilon]^{1/2}$ (allowed indirect Band gap energy in eV)	F(R) vs hυ (band gap energy Irrespective of direct or indirect in eV)
APM	2.60	2.73	2.71
APM/PAni	3.96	3.97	4.01
APM/PNMAni	3.97	4.03	4.05

The band gap energies of APM and composites calculated from UV-DSR spectra have been tabulated in Table VI.4. In all the three cases, the allowed direct band gap energy showed lowest value. The optical band gaps of composites increased considerably compared to APM. The increase in band gap was probably due to the incorporation of polymer chain in APM. For APM, the corresponding wavelength for allowed direct band gap energy and allowed indirect band gap energy and band gap energy irrespective of direct or indirect are 477, 454 and 457 nm respectively. In the case of APM/PAni as the band energy increased with respect to APM, blue shift observed at 313, 312 and 309 nm respectively. In the case of APM/PNMAni also, the corresponding wavelength was observed at 312, 307 and 306 nm respectively indicating shift towards lower wavelength region compared to APM. The increase in band gap energy provides scope for applications in photonic devices like light emitting diodes and laser diodes [38].

VI.7. Removal of Cr(VI) from aqueous solution

The removal hexavalent chromium was done according to the procedure of United States Environment Protection Agency [39]. The efficiency of the synthesized materials to remove Cr(VI) was determined colorimetrically using UV-Vis spectroscopy. Initially the ability of two components of composite, APM and polymer to remove Cr(VI) from aqueous solution was investigated. It was found that, APM was not a good candidate for this purpose. But PAni and PNMAni polymers could remove hexavalent chromium ions completely from aqueous solution upto nine cycles. In the next step the ability of the synthesized composites to remove Cr(VI) was analyzed. In the preliminary studies, APM/PNMAni showed more

potency; therefore detailed investigation was carried out using APM/PNMAni. The Cr(VI) removal studies were carried out using the following chemicals:

- Stock solution of 50 ppm $K_2Cr_2O_7$ solution was prepared by dissolving 0.014 g of $K_2Cr_2O_7$ in 100 ml deionized water.
- Working standard solution of 2 ppm $K_2Cr_2O_7$ solution was prepared by diluting 4 ml of the above stock solution to 100 ml using deionized water.
- Diphenyl carbazide (DPC) solution was prepared by dissolving 0.05 g of DPC in 10 ml acetone.
- 10 % H_2SO_4

VI.7.1. Procedure for Cr(VI) removal

To 10 ml of 2 ppm $K_2Cr_2O_7$ solution, a definite amount of substance (APM/ polymer / composite) was added and stirred using a magnetic stirrer. The contents of the beaker were centrifuged after 60 minutes. 9.5 ml of the centrifugate was collected and pH was adjusted to 2±0.5 using 10% H_2SO_4. DPC (0.2 ml) was added to develop color and the resultant solution was diluted to 10 ml using deionized water. UV-Vis spectra were recorded in the range 200-800 nm to analyze the presence of Cr(VI). This procedure was repeated in all experiments performed in this chapter.

VI.7.2. Cr(VI) removal studies using the components of composites

The Cr(VI) removal capacity of 0.08 g of APM, PAni and PNMAni for 2 ppm solution of Cr(VI) was investigated at pH 5±0.5 (Figure VI.7). The characteristic peak of Cr(VI) was observed at 542 nm. It was observed that PNMAni was most effective in removing Cr(VI)

from an aqueous solution. Therefore, more studies were carried out using PNMAni to understand the nature and mechanism of the removal of Cr(VI) when polymer is used.

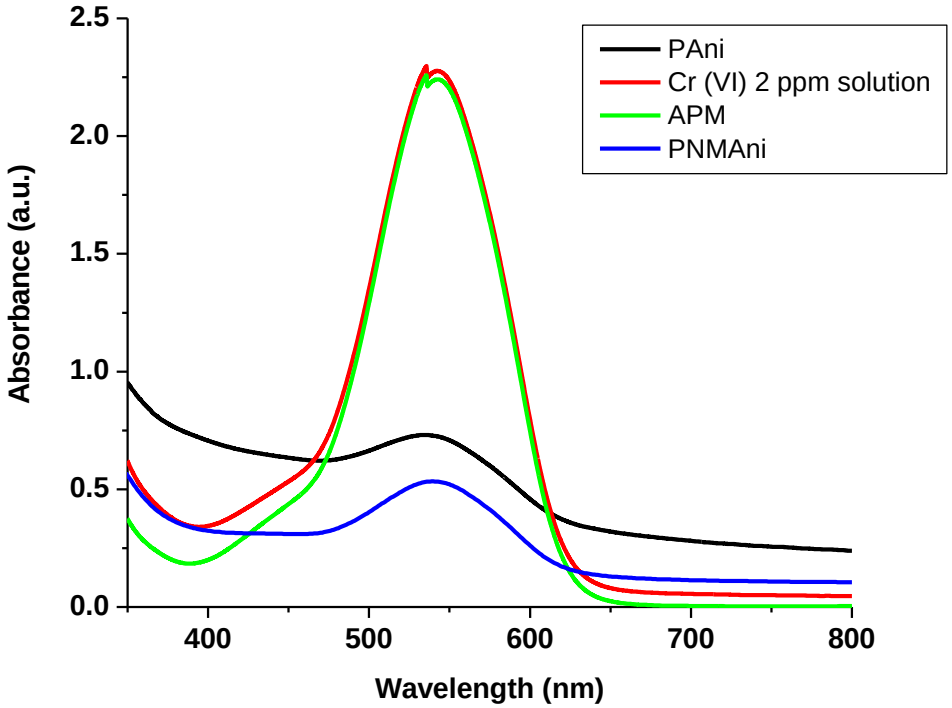

Figure VI.7. The UV-Vis spectra for Cr(VI) removal by PAni, PNMAni and APM; along with 2 ppm Cr(VI) solution.

VI.7.3. Effect of amount of PNMAni

To investigate the effect of amount, different quantities of PNMAni (0.02 g, 0.04 g, 0.06 g, 0.08 g and 0.1 g) was added to 2 ppm solution of Cr(VI) having pH 5±0.5. The above procedure was repeated and the UV-Vis spectra were recorded (refer Figure VI.8). From the UV-Vis data it was concluded that the Cr(VI) removal increases as the amount of polymer increases and maximum removal obtained when 0.1 g of PNMAni was used.

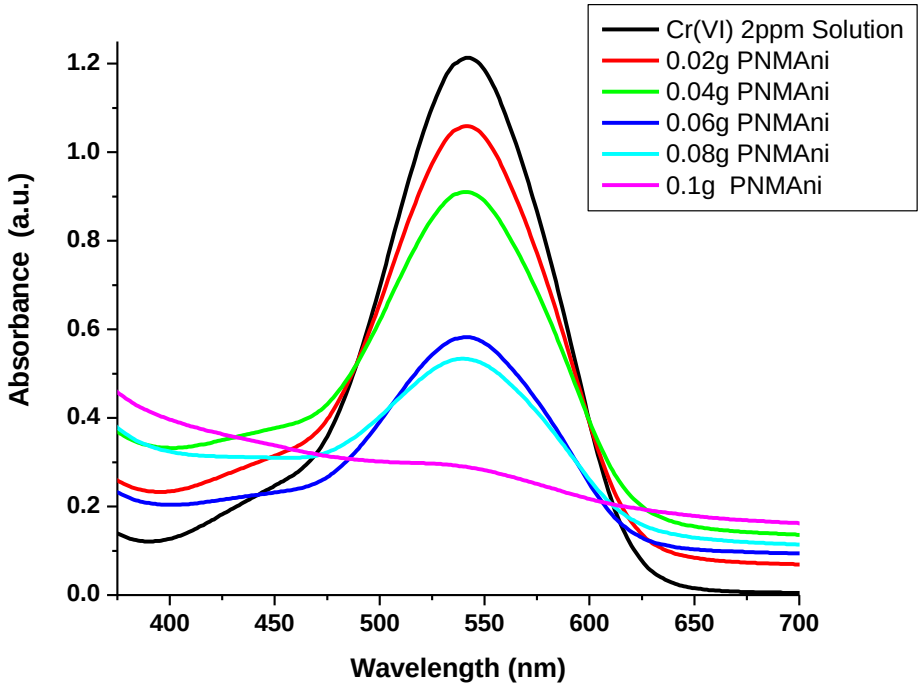

Figure VI.8. The UV-Vis spectra for Cr(VI) removal by PNMAni with varying amount.

VI.7.4. Effect of contact time

To study the effect of contact time between Cr(VI) solution and polymer, 0.1 g of polymer was taken in four different beakers and 10 ml of 2 ppm Cr(VI) solution at pH 5±0.5 was added. The content of first beaker filtered immediately after mixing and considered as zero minutes. The contents of the 2^{nd}, 3^{rd} and 4^{th} beakers were sonicated and filtered at different time intervals i.e. 10 minutes, 20 minutes, 30 minutes and 60 minutes respectively. It was observed that the efficiency of Cr(VI) removal increased when the contact time was increased and maximum removal efficiency was obtained at 60 minutes (refer Figure VI.9).

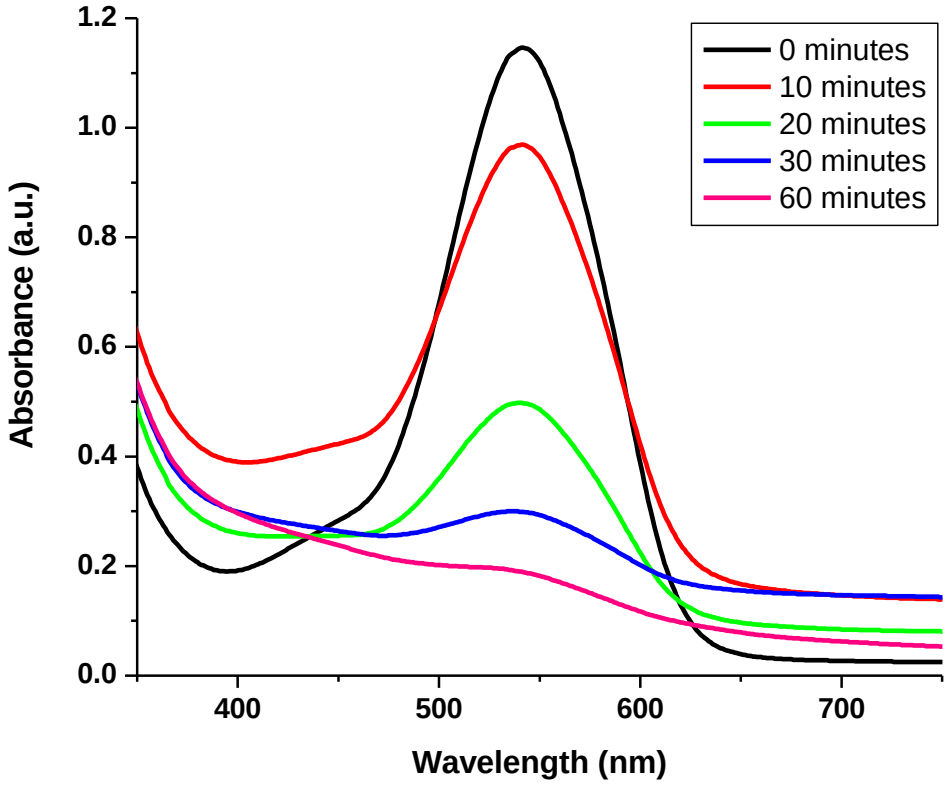

Figure VI.9. The UV-Vis spectra for Cr(VI) removal by PNMAni at different time intervals.

VI.7.5. Cr(VI) removal using APM/PNMAni

APM/PNMAni had selected for Cr(VI) removing studies since it showed good efficiency compared to APM/PAni. In this case, a bluish green coloured solution was obtained after stirring one hour. The content of the beaker was filtered and UV-Vis spectrum of the bluish green solution was recorded. The same procedure was repeated for different pH (pH = 1-5 ±0.5) to understand the effect of pH. The UV-Vis spectrum of this coloured solution exhibited the characteristic absorption peaks of Cr(III) at 430 and 615 nm, indicating the reduction of Cr(VI) to Cr(III) (refer Figure VI.10).

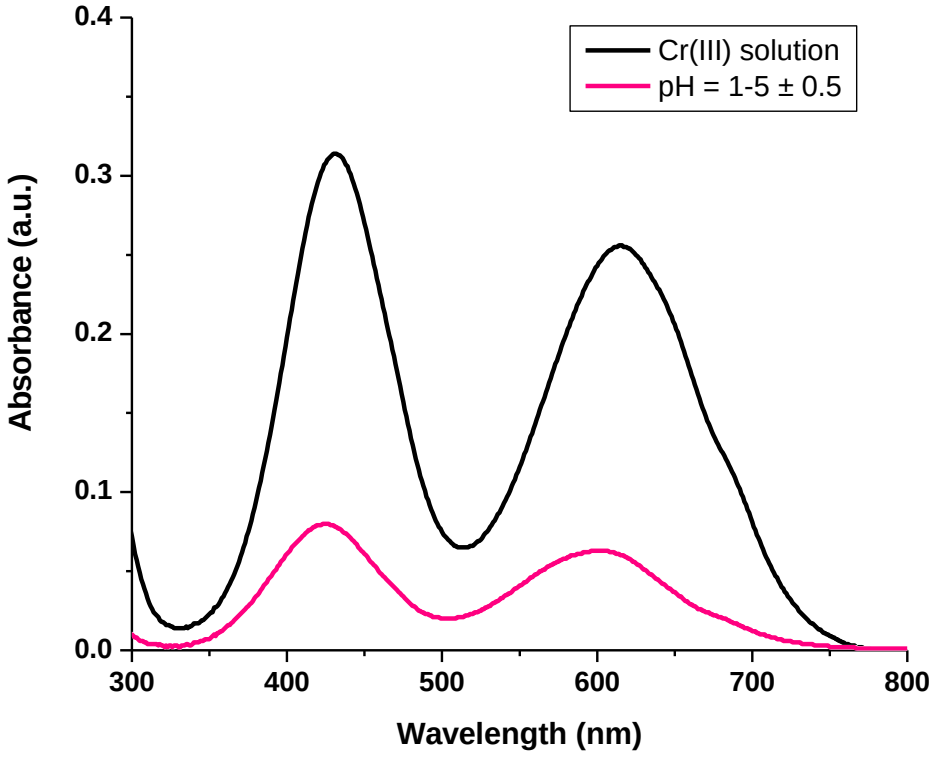

Figure VI.10. The UV-Vis spectra for original Cr(VI) solution and for the solution obtained after adding APM/PNMAni at pH = 1-5 ±0.5.

VI.7.6. Proposed mechanism for Cr(VI) removal

Removal of hexavalent chromium ions has drawn attention of researchers due to its high toxicity and mobility. It is a challenge to remove Cr(VI) ions from industrial waste water. Different materials have been used in the literature for the effective removal of Cr(VI) ions [40-42]. From the above studies it is observed that, Cr(VI) could remove from its 2 ppm aqueous solution with 0.1 g of polymer by one hour of constant stirring. The process of removal could be due to the electrostatic force of attraction between the protonated polymer chain and $Cr_2O_7^{2-}$ anions (as shown in Scheme VI.2).

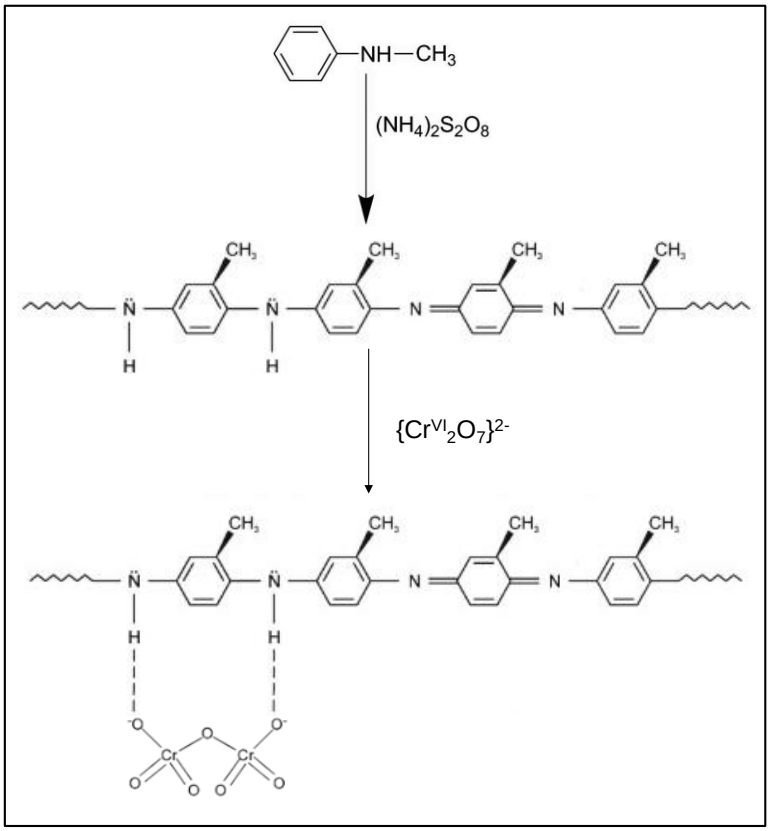

Scheme VI.2. The scheme for the removal of Cr(VI) using poly(N-methylaniline).

On the other hand, the composite acted as a reducing agent for the reduction of toxic Cr(VI) to environmentally benign Cr(III). Earlier Kishore *et. al* [43] have reported the formation of reduced PMo_{12} during the polymerization of aniline using $[H_3PMo_{12}O_{40}]$. The reduced PMo_{12} species generated *in-situ* was utilized for the reduction of metal ions to form metal nanoparticle embedded PAni-PMo_{12} composite. It could be inferred that a similar mechanism was observed herein. Ammonium phosphomolybdate formed in the reaction medium could act as an oxidizing agent and resulted in the polymerization of N-methylaniline, thus forming the composite. The reduced Mo(V) centers in the composite were oxidized to Mo(VI) and in turn reduced Cr(VI) to Cr(III) (refer Scheme VI.3). The CV

results discussed under Section VI.5 also suggested that the redox peaks obtained for APM/PNMAni were corresponding to the one electron transfer.

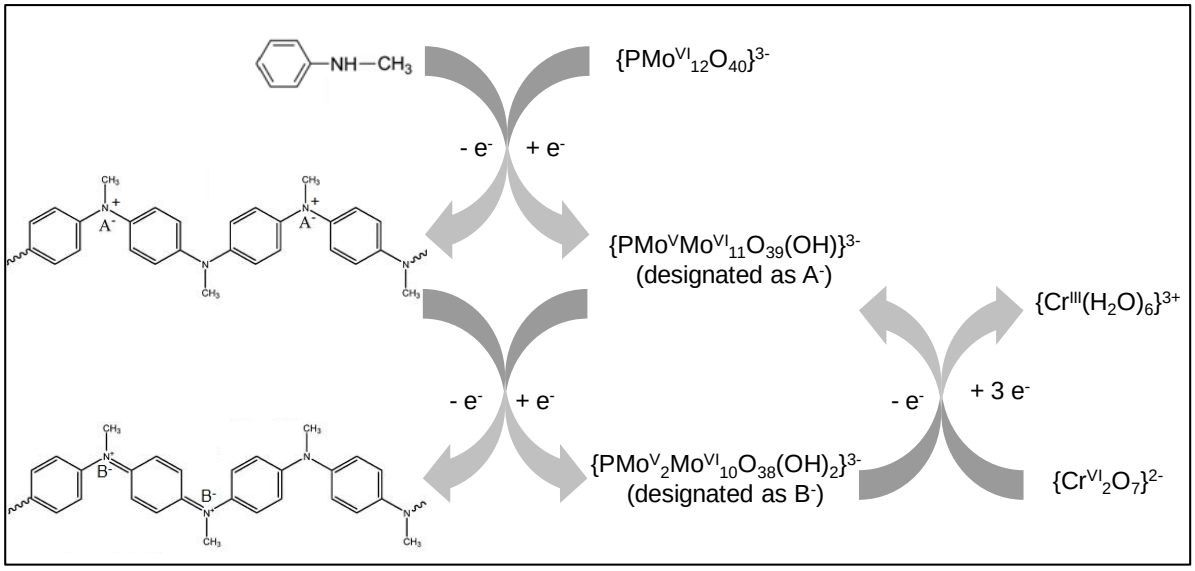

Scheme VI.3. Scheme showing the mechanism for reduction of Cr(VI) to Cr(III) using APM/PNMAni composite.

The reduction of Mo(VI) to Mo(V) during the composite formation was confirmed by recording UV spectrum of the ammonium heptamolybdate solution used for the composite formation and the filtrate collected from the beaker containing the reagents for the composite formation after one hour of stirring (refer Figure VI.11). The broad absorption ~750 nm which is characteristic for the presence of Mo(V) species [43] was obtained for the filtrate collected during composite formation which indicated the reduction of Mo(VI) to Mo(V).

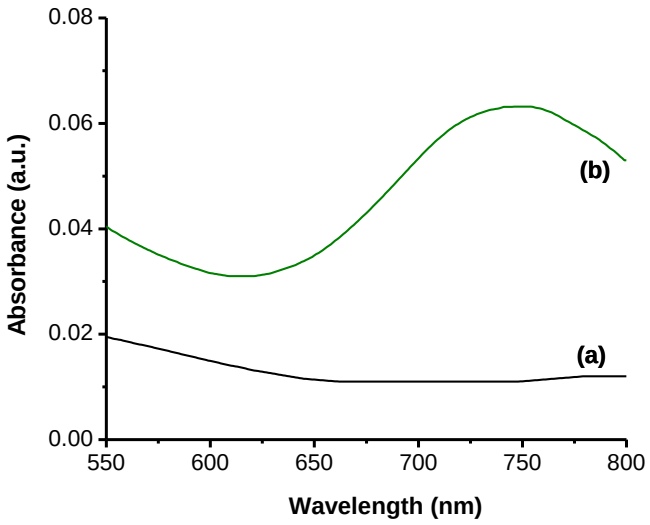

Figure VI.11. UV-Vis spectra of (a) ammonium heptamolybdate solution and (b) filtrate collected during composite formation after stirring one hour.

VI.8. Conclusions

Two polymer composites of APM namely, APM/PAni and APM/PNMAni were synthesized and characterized using FTIR, PXRD and SEM-EDAX. The optical band gap energy of APM and its composites was studied using UV-DRS spectroscopy and it was found that the E_g of the composite materials were higher than that of APM. The electrochemical behavior of APM and its composites was also investigated and APM/PNMAni exhibited highest peak current response as compared to APM and APM/PAni in the presence of a redox species 1 mM $K_4[Fe(CN)_6]$ in 0.1 M KCl indicating its ability to act as a good redox-catalyst. The ability of the synthesized solids to remove toxic Cr(VI) from aqueous medium was investigated. While polymers could removed Cr(VI) via electrostatic interaction between polymeric backbone and dichromate ions; APM/PNMAni could reduce the harmful hexavalent chromium to environmentally benign trivalent chromium species.

References

1. Xie, F.; Ren, J.; Liu, W.; Wang. T.; Yuan, J.; Jiang, X.; Zhang, H. *J. Clust. Sci*. **2018**, 29, 1227-1232.
2. Pathan, S.; Patel, A. *Catal. Sci. Technol*. **2014**, 4, 648-656.
3. Ghalebi, H. R.; Aber, S.; Karimi, A. *J. Mol. Catal. A: Chem*. **2016**, 415, 96-103.
4. Xu, J.; Cao, X.; Xia, J.; Gong, S.; Wang, Z.; Lu, L. *Anal. Chim. Acta* **2016**, 934, 44-51.
5. Lu, L.; Xie, Y. *New J. Chem*. **2017**, 41, 335-346.
6. Wang, Z.; Han, Q.; Xia, J.; Xia, L.; Bi, S.; Shi, G.; Zhang, F.; Xia, Y.; Li, Y.; Xia, L. *J. Electroanal. Chem*. **2014**, 726, 107-111.
7. Li, Z. J.; Zhao, W. J.; Shi, Y.; Ying, Z. P.; Feng, W.; Bai, L. *Compos. Interfaces* **2018**, 25, 809-821.
8. Papagianni, G. G.; Stergiou, D. V.; Armatas, G. S.; Kanatzidis, M. G.; Prodromidis, M. I. *Sens. Actuators, B* **2012**, 173, 346-353.
9. Kim, Y.; Shanmugam, S. *ACS Appl. Mater. Interfaces* **2013**, 5, 12197-12204.
10. Wang, Q.; Liu, E.; Zhang, C.; Huang, S.; Cong, Y.; Zhang, Y. *J. Colloid Interface Sci.* **2018**, 516, 304-311.
11. Hou, L.; Zhang, Y.; Ma, Y.; Wang, Y.; Hu, Z.; Gao, Y.; Han, Z. *Inorg. Chem.* **2019**, 58, 16667-16675.
12. Gong, K.; Liu, Y.; Wang, W.; Fang, T.; Zhao, C.; Han. Z.; Zhai, X. *Eur. J. Inorg. Chem*. **2015**, 2015, 5351-5356.
13. Wang, X.; Wang, J.; Geng, Z.; Qian, Z.; Han, Z. *Dalton Trans*. **2017**, 46, 7917-7925.
14. Abu-Zied, B. M.; Farrag, A. A. A.; Asiri, A. M. *Powder Technol.* **2013**, 246, 643-

649.

15. Lento, J.; Harjula, R. *Solvent Extr. Ion Exch.* **1987**, 5, 343-352.
16. Lopez, R.; Gomez, R. *J. Sol-Gel Sci.Technol*. **2012**, 61, 1-7.
17. Reddy, K. M.; Manorama, S. V.; Reddy, A. R. *Mater. Chem. Phys*. **2003**, 78, 239-245.
18. Wang, Z.; Zhang, R.; Ma, Y.; Zheng, L.; Peng, A.; Fu, H.; Yao, J. *J. Mater. Chem*. **2010**, 20, 1107-1111.
19. Fernandes, D. M.; Freire, C. *ChemElectroChem* **2015**, 2, 269-279.
20. Zheng, H.; Liu, Z.; Huang, D.; Wang, S.; Li, B. *ChemistrySelect* **2017**, 2, 7741-7750.
21. Ding, D.; Zhang, Z.; Chen, R.; Cai, T. *J. Hazard. Mater*. **2016**, 324, 753-761.
22. Park, Y.; Lee, Y. C.; Shin, W. S.; Choi, S. J. *Chem. Eng. J*. **2010**, 162, 685-695.
23. Bhat, A. H.; Bhat, I. U. H.; Khalil, H. P. S. A. *J. Compos. Mater*. **2010**, 45, 39-49.
24. Chen, J.; Dong, L. L.; Feng, W.; Liu, S. L.; Liu, J.; Yang, F. L. *J. Mol. Struct*. **2013**, 1049, 414-418.
25. Matteis, L. D.; Mitchell, S. G.; Fuente, J. M**.** *J. Mater. Chem. B***, 2014**, 2, 7114-7117
26. Holdsworth, A. F.; Eccles, H.; Rowbotham, D.; Bond, G.; Kavi, P. C.; Edge, R. *Separations* **2019**, 6, 1- 9.
27. Sammah, N.; Ghiaci, M. *Ind. Eng. Chem. Res.* **2017**, 56, 10597-10604.
28. Zhang, Z. M.; Li, T. T.; Liu, C. *Appl. Mech. Mater.* **2013**, 395, 415-418.
29. Yang, H.; Xie, Y.; Wang, Y.; Wu, B.; Chen, Y.; Xu, B. *Nano-Structures & Nano-Objects* **2017**, 11, 76-81.

30. Wang, Q.; Liu, E.; Zhang, C.; Huang, S.; Cong, Y.; Zhang, Y. *J. Colloid Interface Sci.* **2018**, 516, 304-311.
31. Li, Z. S.; Lin, S.; Chen, Z. L.; Shi, Y. D.; Huang, X, M. *J. Colloid Interface Sci.* **2012**, 368, 413-419.
32. Ganesan, R.; Gedanken, A. *Nanotechnology* **2008**, 19, 435709.
33. Joseph, J.; Radhakrishnan, R. C.; Johnson, J. K.; Joy, S. P.; Thomas, J. *Mater. Chem*. *Phys*. **2020**, 242, 122488.
34. Nakamoto K **1978** Infrared and Raman spectra of inorganic and coordination compounds (New York: John Wiley & Sons).
35. Yagan, A.; Pekmez, N. O.; Yildiz, A. *J. Electroanal. Chem*. **2005**, 578, 231-238.
36. Jose, J.; Rajamani, A. R.; Anandaram, S.; Jose, S. P.; Peter, S. C.; Sreeja, P. B. *Appl. Organometal. Chem*. **2019**, 5063.
37. Yogan, A. *Int. J. Electrochem. Sci*. **2019**, 14, 2906-2913.
38. Mukherjee, S.; Maiti, R.; Midya, A.; Das, S.; Ray, S. K. *ACS Photonics* **2015**, 2, 760-768.
39. US EPA (United States Environment Protection Agency), **1992**, Method 7196A, Chromium, Hexavalent (Colorimetric).
40. Shakya, A.; Agarwal, T. *J. Mol. Liq*. **2019**, 293, 111497-111507.
41. Xu, D.; Zhu, K.; Zheng, X.; Xiao, R. *Ind. Eng. Chem. Res*. **2015**, 54, 6836-6844.
42. Xing, J.; Zhu, C.; Chowdhury, I.; Tian, Y.; Du, D.; Lin, Y. *Ind. Eng. Chem. Res*. **2018**, 57, 768-774.
43. Kishore, P. S.; Viswanathan, B.; Varadarajan, T. K. *Nanoscale Res. Lett*. **2008**, 3, 14-20.